Solution Space Studies of Optimal Low-Thrust Trajectories in the Circular Restricted Three-Body Problem

Yang Wang[(1)], Xiyun Hou[(1)]

[(1)]Nanjing University
Nanjing, China
Email: yang.wang@nju.edu.cn

***Abstract* – In this work, the structure of the solution space of optimal GTO-Halo trajectories under the Circular Restricted Three-Body Problem is demonstrated by solution curves, consisting of time- and fuel-optimal solutions. The indirect method and the continuation method are used to find solution curves. The Pareto front that balances the transfer time and the fuel cost is further determined and analyzed.**

I. INTRODUCTION

Earth-Moon liberation point orbits (LPOs) such as halo orbits are viable options for scientific explorations. Increasing attention has been paid on transferring from Earth orbits to LPOs using low-thrust propulsion due to its benefits on saving fuel expenditures. The success of SMART-1 mission also validated the feasibility of low-thrust propulsion for transfers in the Earth-Moon system [1]. Although many works have been devoted to solving optimal low-thrust trajectories, the solution space of the optimal low-thrust trajectories has not been fully studied.

In literature, several works have been devoted to study low-thrust trajectories through their solution space. In [2], the solution space was depicted by a large sample of solutions generated by the method that combines the random guess and the gradient-based method, then the near-linear relationship between pairs of optimal initial costate on the Pareto front was observed. In [3], extensive low-thrust trajectories to the lunar capture were searched by reducing and partitioning the search space, and it revealed that the 5:2 resonance is leveraged by many fuel-optimal trajectories before the lunar capture. In [4], massive fuel-optimal trajectories were generated by considering the Sun's perturbation, and the trajectories were classified into six different families by their shapes, transfer time and fuel cost. However, since sample solutions are used to describe the solution space in the above methods, the structure of the solution space is not well demonstrated.

Describing the solution space requires solving many optimal solutions with different transfer time. Numerical methods dedicated to solving the trajectory optimization problem are mainly categorized as direct, indirect and evolutionary methods. Direct methods enable us to solve the problem by transforming it to a nonlinear programming problem, yet a large number of variables are required to be determined [5]. Evolutionary methods can solve the problem without providing the initial guess, but discrete solutions are obtained [6]. Indirect methods enable us to solve the problem with much fewer unknowns, and they converge fast once a good initial guess is provided [5]. Therefore, the indirect method is employed in this study to determine optimal solutions in the solution space.

In this work, the solution space of optimal GTO-Halo trajectories under the Circular Restricted Three-Body Problem (CRTBP) is studied. Instead of describing the solution space by sample solutions, the solution curves consisting of time- and fuel-optimal solutions are used. To effectively find solution curves, multiple time-optimal solutions are solved by using the continuation method first. Then, by gradually increasing the transfer time, the energy-to-fuel-optimal continuation is executed to search for fuel-optimal solutions. Finally, the solution space described by various solution curves is obtained, and the analysis is carried out.

II. PROBLEM STATEMENT

The dynamical equations of the spacecraft under the CRTBP are

$$\dot{\mathbf{x}} = \mathbf{f}(\mathbf{x}, \mathrm{u}, \boldsymbol{\alpha}) \Rightarrow \begin{cases} \dot{\mathbf{r}} = \mathbf{v} \\ \dot{\mathbf{v}} = \mathbf{g}(\mathbf{r}) + \mathbf{h}(\mathbf{v}) + \mathrm{u}\,\dfrac{T_{\max}}{m}\boldsymbol{\alpha} \\ \dot{m} = -u \end{cases} \quad (1)$$

where $\mathbf{r} = [\mathrm{x}, \mathrm{y}, \mathrm{z}]$, $\mathbf{v} = [\mathrm{v}_x, \mathrm{v}_y, \mathrm{v}_z]$ and m are the position vector, the velocity vector, and the mass, respectively; $\mathbf{x} = [\mathbf{r}, \mathbf{v}, \mathrm{m}]$ is the state vector, $u \in [0,1]$ is the thrust throttle factor, $\boldsymbol{\alpha}$ is the thrust direction unit vector, and g_0 is the gravitational acceleration at sea level. Both the maximum thrust $T_{\max}$ and the specific impulse I_{sp} are assumed constant. The expressions of $\mathbf{g}(\mathbf{r})$ and $\mathbf{h}(\mathbf{v})$ are provided in [7].

The solution space is comprised of solution curves shown in Fig. 1. A solution curve is consisted of one time-optimal solution and fuel-optimal solutions with different transfer time. It is desirable to effectively determine the solution curve.

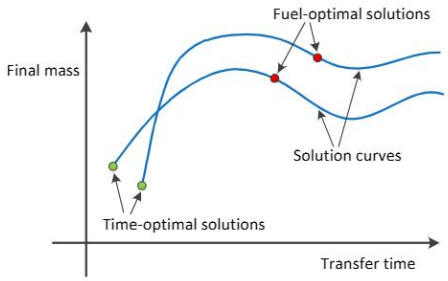

Fig. 1 Solution curves of optimal trajectories.

III. Methodology

A. Time-Optimal Problem

The performance index of the time-optimal problem is

$$J_{\mathrm{TO}} = \int_{t_0}^{t_f} 1 \, dt \tag{2}$$

where t_0 and t_f are the fixed initial time and the free terminal time. The corresponding Hamiltonian function is

$$H = \boldsymbol{\lambda}_r^T \mathbf{v} + \boldsymbol{\lambda}_v^T \left(\mathbf{g}(\mathbf{r}) + \mathbf{h}(\mathbf{v}) + \mathrm{u} \frac{T_{\max}}{m} \boldsymbol{\alpha} \right) - \lambda_m u \frac{T_{\max}}{c} + 1 \tag{3}$$

where $\boldsymbol{\lambda} = [\boldsymbol{\lambda}_r, \boldsymbol{\lambda}_v, \lambda_m]$ is the costate vector.

Based on the Pontryagin Minimum Principle [8], the dynamical equations of the costate is

$$\dot{\boldsymbol{\lambda}} = -\frac{\partial H(\mathbf{x}, \boldsymbol{\lambda}, \mathrm{u}, \boldsymbol{\alpha})}{\partial \mathbf{x}} \tag{4}$$

The optimal u^* and $\boldsymbol{\alpha}^*$ are stated in terms of state and costate are

$$u^* = \begin{cases} 0 & S > 0 \\ 1 & S < 0 \end{cases} \tag{5}$$

and

$$\boldsymbol{\alpha}^* = -\frac{\boldsymbol{\lambda}_v}{\lambda_v} \tag{6}$$

where $\lambda_v = \left\| \boldsymbol{\lambda}_v \right\|$ and S is the switching function as

$$S = -\frac{c}{m} \lambda_v - \lambda_m \tag{7}$$

The motion of the spacecraft is determined by integrating the following state-costate dynamical equations

$$\dot{\mathbf{y}} = \mathbf{F}(\mathbf{y}) \Rightarrow \begin{cases} \dot{\mathbf{r}} = \mathbf{v} \\ \dot{\mathbf{v}} = \mathbf{g}(\mathbf{r}) + \mathbf{h}(\mathbf{v}) - \mathrm{u} \frac{T_{\max}}{m} \frac{\boldsymbol{\lambda}_v}{\lambda_v} \\ \dot{m} = -u \frac{T_{\max}}{c} \\ \dot{\boldsymbol{\lambda}}_r = -G^T \boldsymbol{\lambda}_v \\ \dot{\boldsymbol{\lambda}}_v = -\boldsymbol{\lambda}_r - H^T \boldsymbol{\lambda}_v \\ \dot{\lambda}_m = -u \lambda_v \frac{T_{\max}}{m^2} \end{cases} \tag{8}$$

where $\mathbf{y} = [\mathbf{x}, \boldsymbol{\lambda}]$, $G(\mathbf{r}) = \partial \mathbf{g}(\mathbf{r}) / \partial \mathbf{r}$ and $H(\mathbf{v}) = \partial \mathbf{h}(\mathbf{v}) / \partial \mathbf{v}$.

The initial condition is

$$\mathbf{x}(t_0) = \mathbf{x}_0 \tag{9}$$

The terminal conditions are

$$\mathbf{r}(t_f) = \mathbf{r}_{f,} \quad \mathbf{v}(t_f) = \mathbf{v}_{f,} \tag{10}$$

The transversality condition for the free final mass is

$$\lambda_m(t_f) = 0 \tag{11}$$

The Hamiltonian constraint at the terminal time is

$$H(t_f) = 0 \tag{12}$$

Remark 1: Let $\boldsymbol{\varphi}(t_0, t_f, [\mathbf{r}_f, \mathbf{v}_f, m_f, \boldsymbol{\lambda}_{rf}, \boldsymbol{\lambda}_{vf}, \lambda_{mf} = 0])$ be the solution of Eq. (8) with u^* in Eq. (5) integrated backward from the terminal time t_f to the initial time t_0, the time-optimal problem is to find the optimal $[\boldsymbol{\lambda}_{rf}^*, \boldsymbol{\lambda}_{rf}^*, m_f^*, t_f^*]$ such that $\boldsymbol{\varphi}(t_0, t_f, [\mathbf{r}_f, \mathbf{v}_f, m_f^*, \boldsymbol{\lambda}_{rf}^*, \boldsymbol{\lambda}_{vf}^*, 0])$ satisfies Eqs. (9)-(12).

It is known that multiple time-optimal solutions with different revolutions exist for the orbital transfer problem [9]. It is essential to employ an effective method to search multiple time-optimal solutions. As shown in Fig. 2, starting from the first solution, the continuation by clockwise rotating the line of perigee is executed [9]. The second solution is then found once the line of perigee is rotated by one revolution. In this case, the second solution has one more revolution than the first solution. The counterclockwise rotation of the line of perigee can be executed by searching for local solutions with fewer revolutions.

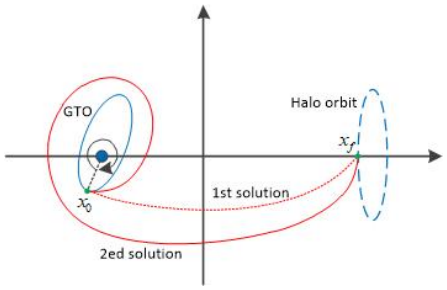

Fig. 2 Continuation on the line of perigee.

B. Fuel-Optimal Problem

The performance of the fuel-optimal problem is

$$J_{\mathrm{FO}} = \frac{T_{\max}}{c} \int_{t_0}^{t_f} u \, dt \tag{13}$$

Since the fuel-optimal problem is difficult to solve directly by zero-finding methods [10], the energy-to-fuel-optimal continuation is employed, with the performance as [10]

$$J = \frac{T_{\max}}{c} \int_{t_0}^{t_f} \left[u - \varepsilon u (1-u) \right] dt \tag{14}$$

The Hamiltonian function of the energy-to-fuel-optimal problem is

$$H=\boldsymbol{\lambda}_r^T\mathbf{v}+\boldsymbol{\lambda}_v^T\left(\mathbf{g}(\mathbf{r})+\mathbf{h}(\mathbf{v})+\mathrm{u}\frac{T_{\max}}{m}\boldsymbol{\alpha}\right)-\lambda_m u\frac{T_{\max}}{c}+\frac{T_{\max}}{c}\left[u-\varepsilon u(1-u)\right] \tag{15}$$

The u^* is stated in terms of S_ε and ε is

$$u^*=\begin{cases}0 & S_\varepsilon>\varepsilon\\ 1 & S_\varepsilon<-\varepsilon\\ (\varepsilon-S_\varepsilon)/(2\varepsilon) & S_\varepsilon\le\|\varepsilon\|\end{cases} \tag{16}$$

where

$$S_\varepsilon=-\frac{c}{m}\lambda_v-\lambda_m+1 \tag{17}$$

Remark 2: Let $\boldsymbol{\varphi}(t_0,t_f,[\mathbf{r}_f,\mathbf{v}_f,m_f,\boldsymbol{\lambda}_{rf},\boldsymbol{\lambda}_{vf},\lambda_{mf}=0])$ be the solution of Eq. (8) with u^* as in Eq. (16) integrated backward from the terminal time t_f to the initial time t_0, the fuel-optimal problem is to find the optimal $[\boldsymbol{\lambda}_{rf}^*,\boldsymbol{\lambda}_{rf}^*,m_f^*,t_f^*]$ such that $\boldsymbol{\varphi}(t_0,t_f,[\mathbf{r}_f,\mathbf{v}_f,m_f^*,\boldsymbol{\lambda}_{rf}^*,\boldsymbol{\lambda}_{vf}^*,0])$ satisfies Eqs. (9)-(11).

Suppose that the maximum value of S for the time-optimal solution is denoted as $S_{\max,\mathrm{TO}}$, and define

$$\gamma_{\mathrm{EO}}=\frac{-2}{S_{\max,\mathrm{TO}}},\quad \gamma_{\mathrm{FO}}=\frac{-1}{S_{\max,\mathrm{TO}}} \tag{18}$$

Then the optimal costates to the energy- and fuel-optimal problems with the minimum transfer time are

$$\lambda_{\mathrm{EO}}^*=\gamma\,\lambda_{\mathrm{TO}}^*,\quad \gamma>\gamma_{\mathrm{EO}} \tag{19}$$

$$\lambda_{\mathrm{FO}}^*=\gamma\,\lambda_{\mathrm{TO}}^*,\quad \gamma>\gamma_{\mathrm{FO}} \tag{20}$$

The Eqs. (19) and (20) can be used to connect the time-optimal solution to the energy- and fuel-optimal solutions with the minimum transfer time. The indirect method in [7] featuring analytic gradients is applied to execute the energy-to-fuel-optimal continuation. This method has the advantage to determine the fuel-optimal solution without providing the thrust sequence a priori.

IV. Simulations

The simulation example from [7] is employed, where the initial point is set to be the perigee of a specified GTO and the terminal point is set to be on the Halo orbit. The thrust value $T_{\max}=10N$ is employed to carry out simulations.

A. Multiple time-optimal solutions

Ten time-optimal solutions are found. Their projections on the plane with the transfer time and the final mass as the axes are shown in Fig. 3, where the solution obtained in [7] is pointed out. It can be seen that the optimal transfer time and the final mass vary linearly in this example. The best time-optimal solution obtained in this work is about 6.7168 days, shorter than the solution in [7] which is 7.8549 days. The best time-optimal trajectory is shown in Fig. 4. Let the revolution be the times that the trajectory transverses the Poincare section $\Sigma=\{y=0,x<-\mu\}$. The best time-optimal trajectory completes the transfer with 4 revolutions, while the solution in [7] requires 7 revolutions. The corresponding variation of the switching function is shown in Fig. 5.

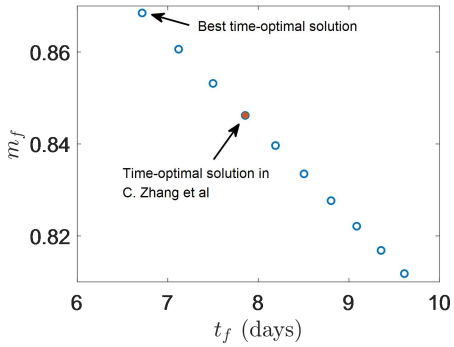

Fig. 3 Time-optimal solutions.

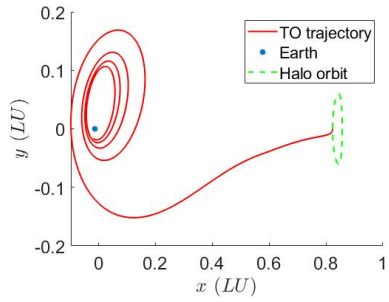

Fig. 4 Time-optimal trajectory of the best solution.

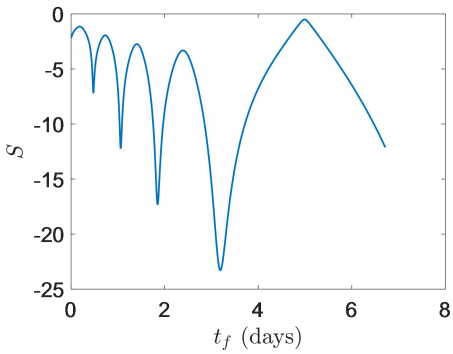

Fig. 5 Variation of the time-optimal switching function.

B. Solution space

Ten solution curves are solved and their projections on the plane with the transfer time and the final mass as the axes are shown in Fig. 6. Instead of the discrete sample solutions, the structure of the solution space that is comprised of solution curves with different revolutions is clearly demonstrated.

The Pareto front that balance the transfer time and the fuel cost is shown as the blue line in Fig. 6. The fuel-optimal solution in [7] is shown to be located on the Pareto front. Within 30 days of the maximum transfer time, it is found that fuel-optimal trajectories with

revolutions higher than eight have no benefits from the viewpoint of the Pareto front. A sample solution on the Pareto front is shown in Fig. 7.

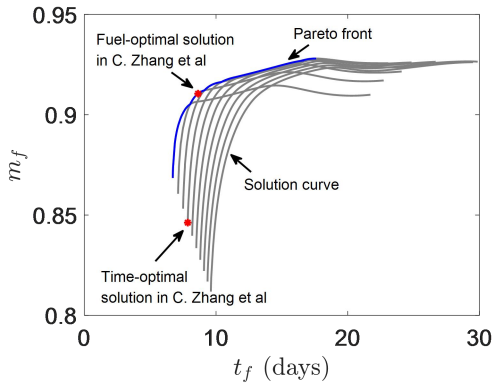

Fig. 6 Solution space and Pareto front (blue line)

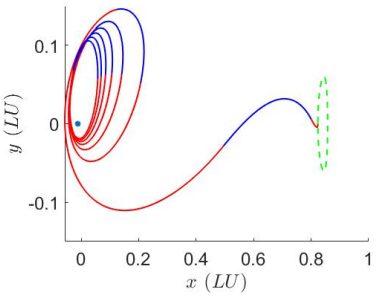

Fig.7 Sample fuel-optimal trajectory on the Pareto front. Red line: thrust arc, blue line: coast arc.

In [2], a near-linear relationship was observed between pairs of the Pareto optimal initial costates. The relationship is also tested in our simulation examples, and the results are shown in Figs. 8-9. It is found that the near-linear relationship obeys for most solutions except several solutions at the beginning of the first solution curve.

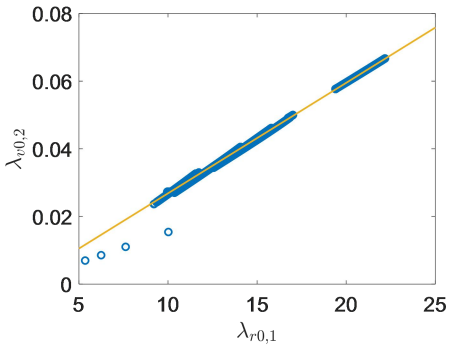

Fig.8 Relationship of optimal initial costates $\lambda_{r0,1}$ and $\lambda_{v0,2}$ on the Pareto front.

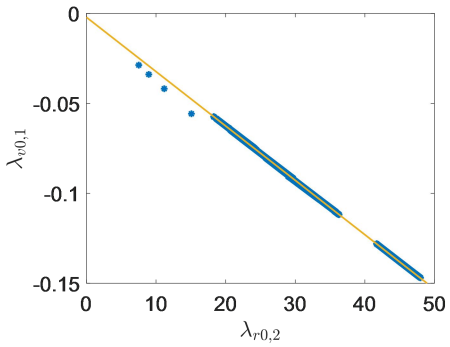

Fig.9 Relationship of optimal initial costates $\lambda_{r0,2}$ and $\lambda_{v0,1}$ on the Pareto front.

V. Conclusion

The solution space of optimal GTO-Halo trajectories is studied. Differently from existing works which describe the solution space using sample solutions, this work depicts the solution space by solution curves. As a result, the structure of the solution space is well demonstrated. The Pareto front that balances the transfer time and the fuel cost is accurately determined. It shows that within 30 days of maximum transfer time, fuel-optimal trajectories with revolutions higher than eight have no benefits from the viewpoint of the Pareto front in the simulation example.

VI. Acknowledgement

Y.W. thanks the support from China Postdoctoral Science Foundation (No. 2023M741638). X.H. thanks the support from National Natural Science Foundation of China (No. 12233003).

VII. References

[1] Rathsman P, Kugelberg J, Bodin P, et al, "SMART-1: Development and lessons learnt", *Acta Astronautica*, vol. 57, no. 2-8, 2005, pp. 455-468.

[2] R. Russell, "Primer Vector Theory Applied to Global Low-Thrust Trade Studies", *Journal of Guidance, Control, and Dynamics*, vol. 30, no. 2, 2007, pp. 460-472.

[3] K. Oshima, S. Campagnola, and T. Yanao, "Global Search for Low-Thrust Transfers to the Moon in the Planar Circular Restricted Three-Body Problem", *Celestial Mechanics and Dynamical Astronomy*, vol. 128, 2017, pp.303-322.

[4] D. Perez-Palau and R. Epenoy, "Fuel Optimization for Low-Thrust Earth-Moon Transfers via Indirect Optimal Control", *Celestial Mechanics and Dynamical Astronomy*, vol. 130, 2018, p. 12.

[5] F. Topputo, C. Zhang, "Survey of direct transcription for low-thrust space trajectory

optimization with applications", *Abstract and Applied Analysis*, vol. 2014, 2014.
[6] B. Conway, "A survey of methods available for the numerical optimization of continuous dynamic systems", *Journal of Optimization Theory and Applications*, vol. 152, no. 2, pp. 271-306.
[7] C. Zhang, F. Topputo, F. Bernelli-Zazzera and Y. Zhao, "Low-Thrust Minimum-Fuel Optimization in the Circular Restricted Three-Body Problem", *Journal of Guidance, Control, and Dynamics*, vol. 38, no. 8, 2015, pp. 1501-1510.
[8] Bryson, A., Ho, Y.-C.: Applied Optimal Control: Optimization, Estimation and Control. Taylor & Francis, New York (1975).
[9] Caillau, J.-B., Farres, A.: On Local Optima in Minimum Time Control of the Restricted Three-Body Problem, pp. 209–302. Springer, 2016.
[10] Bertrand, R., and Epenoy, R., "New Smoothing Techniques for Solving Bang–Bang Optimal Control Problems – Numerical Results and Statistical Interpretation, " Optimal Control Applications and Methods, vol. 23, no. 4, 2002, pp. 171–197.